

# Study on the Influence of Thermal Characteristics of Hyperbranched Polyurethane Phase Change Materials for Energy Storage

Qi Cao, Li Liao, Haili Xu

Key Laboratory of Environmentally Friendly Chemistry and Applications of Ministry of Education, Xiangtan University, Xiangtan, Hunan Province 411105, People's Republic of China

Received 21 December 2008; accepted 19 August 2009

DOI 10.1002/app.31311

Published online 7 October 2009 in Wiley InterScience (www.interscience.wiley.com).

**ABSTRACT:** A series of hyperbranched polyurethane (HB-PU) phase change induced energy storage materials were prepared by polyethylene glycol (PEG), methylene diphenyl 4,4'-diisocyanate (MDI), and hyperbranched polyester polyalcohol via a two-step process. The influence of thermal characteristics of HB-PU was investigated using differential scanning calorimetry (DSC) and wide-angle X-ray diffraction (WAXD). It has been found that the thermal characteristics of HB-PU are affected by some factors. Such as the molecular weight and content of soft segment, once the  $M_n$  of PEG soft segments is larger than the critical  $M_n$  (2000 g/mol), both the phase change enthalpy and

temperature increase as  $M_n$  of PEG soft segment and soft segment content (SSC) increase. The influence of the microstructure of hard segment originates from diisocyanate and hyperbranched polyester polyalcohol, HB-PUs with regular microstructure and lower generation of hyperbranched polyester polyalcohol have high energy storage capability. Furthermore, the conditions of measurement affect the thermal characteristics of materials. © 2009 Wiley Periodicals, Inc. *J Appl Polym Sci* 115: 2228–2235, 2010

**Key words:** hyperbranched polyurethane; thermal characteristics; differential scanning calorimetry (DSC)

## INTRODUCTION

Segmented polyurethane has received growing interest in the last few years. Most of the studies focused on the thermoplastic elastomeric function. These segmented polyurethanes usually do not have energy storage characteristic because of the poor crystallizability of the soft segments. As for phase change induced energy storage materials, the energy change usually arises from the change of entropy of materials. Because the entropy number is a measurement of randomness, entropy number increases as the randomness increases. Therefore, the entropy number is smaller at ordered state than at disordered state for a phase change induced energy storage material. Hyperbranched polyurethane (HB-PU), prepared by using hyperbranched polyester polyalcohol as chain extender, has shown to be a kind of phase change induced energy storage material. The PEG soft segment of the HB-PU is crystallizable. The transition of PEG soft segment of HB-PU from crystalline morphology to amorphous morphology leads to the storage and release of energy. In fact, high degree of crystallinity of soft segment is necessary for HB-PU to have the characteristic of energy storage.

HB-PUs have soft PEG segments and hard segments formed from isocyanate and hyperbranched polyester polyalcohol extender. The hard segments can gather together to form hard segment microdomains due to the hydrogen-bonding interaction. These hard segment microdomains behave as physical crosslink point and filling materials, which makes HB-PU to remain in solid state when soft segment melt to amorphous morphology. However, the hard segment of HB-PU are dispersed in soft segment domains, it is unclear in what condition the gathering of hard segments can form enough physical crosslink points to make sure that HB-PU can remain in solid state during phase change. Therefore, it is worthy of studying the thermal property of various HB-PUs.

In this article, we discuss the effects of the molecular weight of soft segment, the types of hard segment and the measure conditions on thermal of HB-PU. In addition, the influence of thermal property of HB-PU on energy storage is also investigated.

## EXPERIMENTAL

### Materials

Polyethylene glycol (PEG,  $M_n = 600, 1000, 2000, 4000, 6000, 10,000, 20,000$  g/mol, a chemically pure reagent, from Tianjin Chemical Regent Co., China).

Correspondence to: Q. Cao (wjcaoqi@163.com).

Methylene diphenyl 4,4'-diisocyanate (MDI, from Wanhua Chemical Reagent Co., China).

Toluene-2,4-diisocyanate (TDI, chemically pure reagent, from Tianjin Chemical Reagent Co., China).

Boltorn® H20 (Second generation,  $M_w = 1750$  g/mol, hydroxyl number equals 480–510 mg KOH/g, Sweden) and Boltorn® H30 (Third generation,  $M_w = 3500$  g/mol, hydroxyl number equals 480–510 mg KOH/g, Sweden) were purchased from Rerstorp Specialty Chemicals.

*N,N'*-dimethyl formamide (DMF, from Shantou Guanghua Chemical Reagent Co., China).

All of the reagents were dried and purified before use.

### Synthesis of HB-PU

PEG 10 g (0.0017 mol) and excess MDI 1.6 g (0.0064 mol) in freshly distilled DMF (30 mL) solutions were mixed and stirred at 80°C under vacuum for 3 h. Then a predetermined amount of hyperbranched polyester polyalcohol (Boltorn® H20 or Boltorn® H30) in dried DMF was added to the stirring reaction mixture. The amount of —NCO groups of MDI is kept to equal to the total amount of —OH groups in both PEG and Boltorn® H20 (or Boltorn® H30). After stirring for another 2 h, the reaction mixture was casted onto a glass pan. Polymer films with thickness of 0.2–1.0 mm were obtained after curing at 80°C for 24 h. The samples were kept in vacuum at room temperature for 2 weeks before testing.

Five sorts of HB-PU were produced with different molecule weight of soft segments (600–20,000 g/mol). The mass fraction of soft segments alters from 60 to 90 wt %. HB-PU with different types of hard segments were prepared using similar procedure as mentioned earlier.

### DSC analysis

Phase change temperature and phase change enthalpy was performed on a DSC-7 differential scanning calorimetry equipment (PE Company). The mass of test sample is ~5 mg; the heating rate is 20°C/min; and the scanning temperature ranges from –50 to 200°C. In the first scanning, test sample is heated to 200°C, and kept at this temperature for 5 min, then cooled to –50°C. The second scanning is the same as the first one. The data from second scanning is used for calculations.<sup>1</sup> Through the second curve data, the crystallinity of test sample is calculated using following equation:

$$X_{C,PEG}(\%) = \frac{\Delta H_{m-PEG'}}{\Delta H_{m-PEG}^0} \times 100$$

where  $\Delta H_{m-PEG}^0$  is the heat of melting of 100% crystalline PEG (using heat of fusion of 197 J/g for

PEG),<sup>2</sup>  $\Delta H_{m-PEG}$  is the heat of melting of the polymer under investigation, determined by differential scanning calorimetry (DSC).

## RESULTS AND DISCUSSION

### The influence of soft segment on thermal property of HB-PU

Relationship between molecule weight of PEG and thermal property of HB-PU

PEG is made up of  $(-\text{CH}_2-\text{CH}_2-\text{O}-)_n$ , which is a di-hydroxyl terminated polymer. The melt temperature ( $T_m$ ) and the melt enthalpy ( $\Delta H_m$ ) of PEG are dependant on the molecule weight of PEG when the PEG molecule weight is <20,000 g/mol. Therefore, the  $T_m$  and  $\Delta H_m$  of PEG segments in HB-PU can be tailored by manipulating the molecule weight of used PEG. As such, HB-PU with different phase change temperatures can be obtained by the reaction of a series of PEG having different molecule weights with diisocyanates and hyperbranched polyesters.

PEG test samples with different  $M_n$  exhibited obviously singlet in both the heating and cooling DSC curves. The melting points and melt enthalpy numbers of PEG with various  $M_n$  were shown in Table I. As shown in Table I,  $T_m$  and  $\Delta H_m$  of PEG depended on  $M_n$  in heating scanning.  $\Delta H_m$  increased quickly as  $M_n$  increased when  $M_n$  of PEG was <4000; once  $M_n$  exceeded 4000,  $\Delta H_m$  kept an approximate constant value; when  $M_n$  attained 10,000,  $\Delta H_m$  reached the maximum value; and then  $\Delta H_m$  decreased a little when  $M_n$  was over 10,000. Similarly,  $T_m$  increased quickly as  $M_n$  increased before  $M_n$  was above 4000. In the cooling scanning, the situation is similar.

Relationship between soft segment and energy storage property of HB-PU

A series of HB-PU materials that have different soft segment length (SSL) and soft segment content (SSC) were prepared by PEG with various  $M_n$  as soft segment and MDI-H20 as hard segment, Figure 1 is the DSC curves of HB-PU with various  $M_n$  of PEG (SSC is 80 wt %). The heat flow of DSC analysis can be described by the equation that derived from a simple equation based on thermodynamic theory, and it has been reported in other literature.<sup>3</sup> As shown in Figure 1(a), the DSC curves of HB-PU with PEG 600 or PEG 1000 soft segments have not shown any peak. This indicates that HB-PU with PEG 600 or PEG 1000 soft segments are not crystalline at all, although PEG 600 and PEG 1000 themselves are highly crystalline. When the  $M_n$  of PEG segments is 2000 or >2000, HB-PU appear quite strong fusion peaks in the range from 57 to 69°C.

TABLE I  
Thermal Properties of PEG Measured by DSC Analysis

$M_n$	600	1000	2000	4000	6000	10,000	20,000
$T_m$ (°C)	18.5	41.2	60.1	64.2	67.2	67.8	68.7
$\Delta H_m$ (J/g)	121.1	137.3	142.0	152.4	155.1	177.2	159.5
$T_c$ (°C)	6.9	13.8	27.2	33.8	34.6	36.8	37.6
$\Delta H_c$ (J/g)	116.1	134.2	136.2	150.5	152.0	168.9	155.2

The  $T_m$  and  $\Delta H_m$  of soft segments increase rapidly as  $M_n$  of soft segments increases until  $M_n$  attains to a certain number. As shown in Figure 1(b), the crystallizing enthalpy ( $\Delta H_c$ ) and crystallizing point ( $T_c$ ) of HB-PU are also dependant on the  $M_n$  of PEG soft segments. When the  $M_n$  of soft segments is over 2000, soft segments of HB-PU can crystallize perfectly at room temperature. Rather large phase change of soft segments of HB-PU leads to significant heat absorption or radiation, which makes HB-PU very good heat storage material. Summarizing

the discussion above, there is a critical  $M_n$  (2000 g/mol) of soft segments for HB-PU phase change induced energy storage materials. HB-PU will not have the heat storage property until the  $M_n$  of PEG soft segments is larger than the critical  $M_n$  (2000 g/mol). When the  $M_n$  of PEG soft segments is larger than the critical  $M_n$  (2000 g/mol), the phase change enthalpy and the phase change temperature increase rapidly as  $M_n$  of PEG soft segments increases, until PEG chain of soft segments becomes so long that longer chain almost cannot enhance the degree of crystallinity of PEG soft segments in HB-PU.

To further understand the influence of soft segments on heat storage property of HB-PU, the effect of SSC on the transition temperature and the enthalpy of HB-PU was investigated. As shown in Figures 2 and 3, when  $M_n$  of PEG is greater than the critical  $M_n$  (2000 g/mol), both the phase change enthalpy and phase change temperature of HB-PU decrease as SSC decreases. The phase change enthalpy varies sharper than phase change temperature. This can be explained by the phase change of PEG soft segments in HB-PU. Hard segments do not contribute to the phase change enthalpy. Once

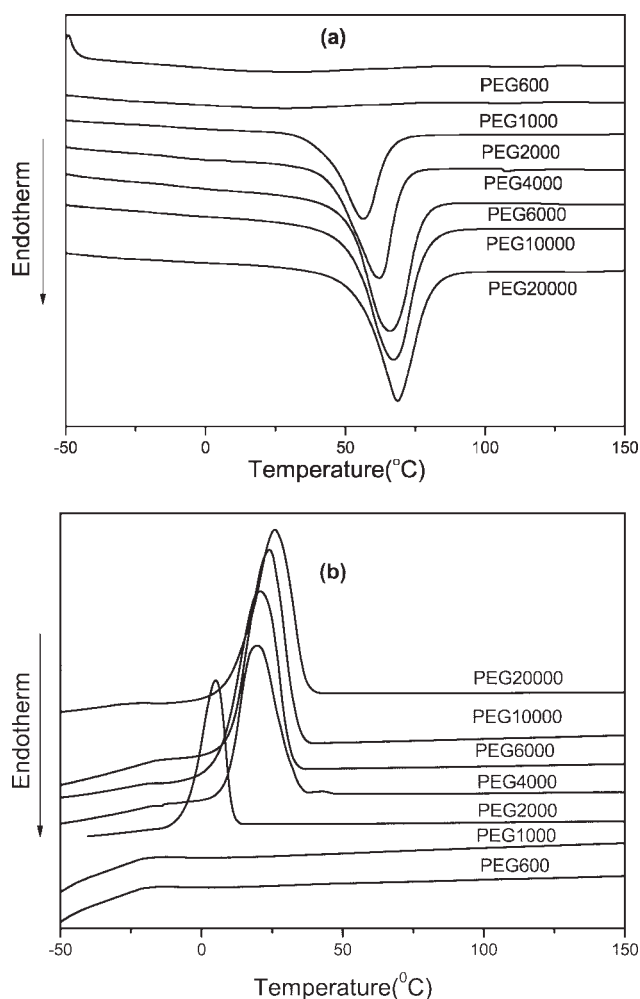


Figure 1 DSC curves for HB-PU with various  $M_n$  of PEG: (a) Heating curves and (b) cooling curves.

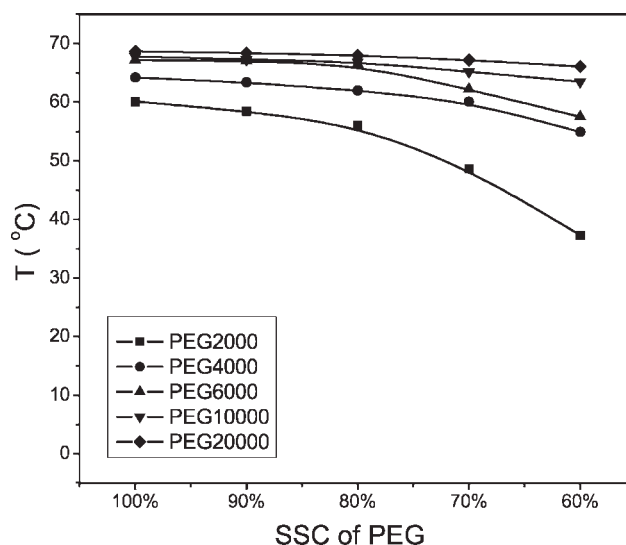
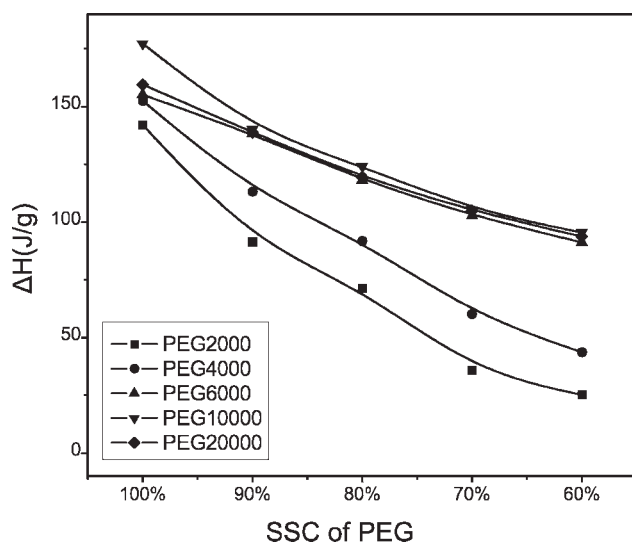


Figure 2 Relationship curves between the transition temperature and the SSC of PEG.



**Figure 3** Relationship curves between the enthalpy and the SSC of PEG.

SSC in HB-PU decreases, portions of phase change domains in unit mass decrease too. This results in the decline of phase change enthalpy of HB-PU energy storage polymer. However, the reason is different for the phenomenon that the phase change temperature decreases with SSC decreasing. Because the hard segments of HB-PU are not crystallizable, the phase change temperature is determined by the soft PEG segments of HB-PU.  $T_m$  and  $T_c$  of PEG increase with increasing  $M_n$  of PEG, so the phase change temperature of HB-PU also increases with increasing  $M_n$  of soft PEG segment, as shown in Figure 2. It is noteworthy that the crystallization of soft segments is restrained by hard segments in HB-PU. Hard segments and soft segments of HB-PU are thermodynamically incompatible and form microdomains separately. PEG soft segment chain units in the interface sections between the hard segment microdomains and soft segment microdomains cannot enter the soft segment crystalline domains freely, therefore, the number of crystallizable PEG soft segment chain units reduced. It has similar effect to the decrease of  $M_n$  of crystallizable PEG soft segment. Consequently, both the enthalpy and temperature of phase change decrease as the SSC decreases.

To illuminate the influence of  $M_n$  of PEG soft segments on energy storage property of HB-PU, the effect of SSL on transition temperature and the enthalpy of HB-PU was investigated too. As shown in Figures 4 and 5, the relationship of the transition enthalpy and the transition temperature with the  $M_n$  of the PEG segments in HB-PU was similar to that of pure PEG. The enthalpy increased as  $M_n$  of soft segments increased, and reached its maximum when  $M_n$  of PEG segment reached 10,000, then it dropped

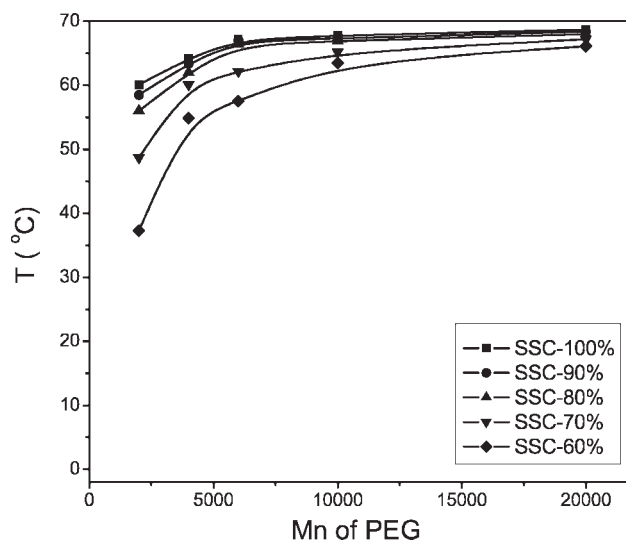


**Figure 4** Relationship curves between the transition temperature and the  $M_n$  of PEG.

slightly as  $M_n$  of PEG segment exceeded 10,000. After  $M_n$  of PEG segment was above 10,000, the transition temperature increased slightly as  $M_n$  of PEG segment increased. When  $M_n$  of pure PEG is low, the number of terminal groups in pure PEG is larger. This reduces the crystalline integrity of pure PEG because the terminal groups are impurities. Because the terminal groups and the crystalline defect decrease as  $M_n$  of pure PEG increases, the crystallinity and the enthalpy increase with increasing  $M_n$  of pure PEG. Once  $M_n$  of pure PEG reaches a critical value, intermolecular entanglement increase. As a result, the crystallinity and the enthalpy decrease although the number of terminal groups decreases.

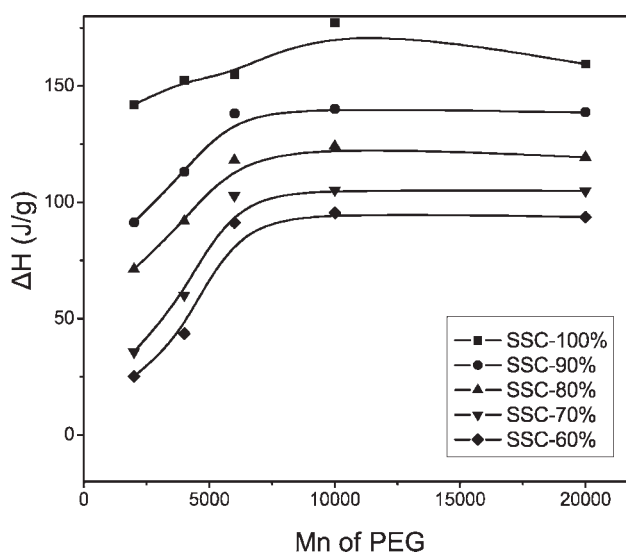


**Figure 5** Relationship curves between the enthalpy and the  $M_n$  of PEG.

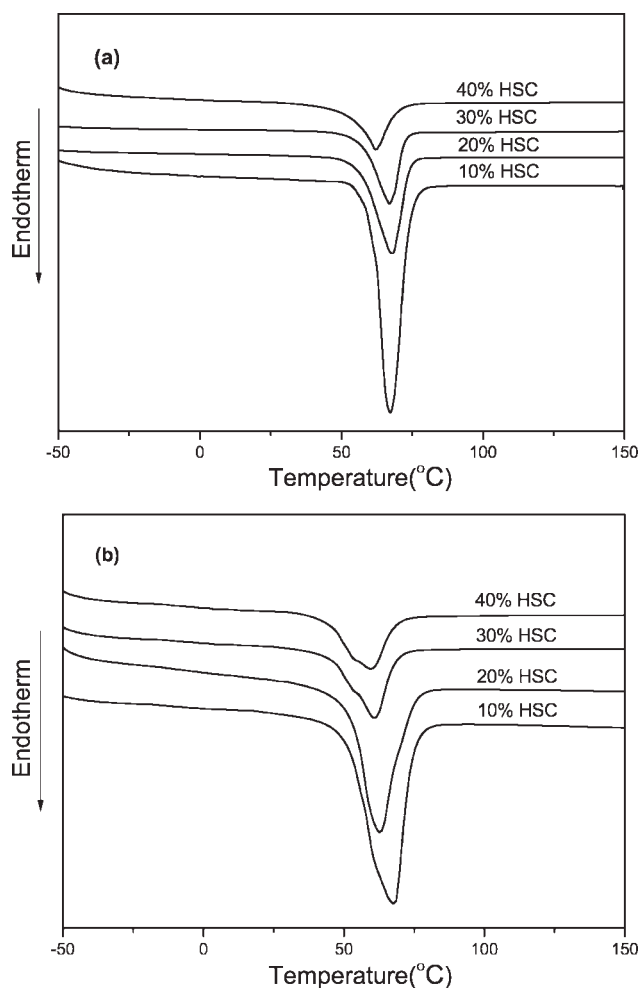


**Figure 6** DSC curves for HB-PU with various hard segment content (HSC): (a) MDI-HB-PU and (b) TDI-HB-PU.

### Influence of hard segment on thermal property of HB-PU

Hard segments have great influence on the properties of solid–solid phase change of HB-PU. Hard segments in HB-PU assemble into microdomains and form physical crosslinked network. A number of works on the phase separation of thermoplastic polyurethane elastomers have been published.<sup>4–14</sup> In block polyurethane elastic system, the solubility parameter is lower in flexible soft segment than in rigid hard segment, the two segments are incompatible, and, therefore, the two segments are separated into two phases. Generally, the microphase separation is more pronounced when PU has relative rigid hard segments, high hard segment content (HSC), or longer soft segments.

Hard segment of HB-PU is made up of diisocyanate and hyperbranched polyester polyalcohol. Therefore, both the diisocyanate and hyperbranched polyester polyalcohol will affect the heat storage property of HB-PU.

### Influence of diisocyanate type on heat storage property

To investigate the influence of diisocyanate on the heat storage property of HB-PU, two families of HB-PU were synthesized from PEG ( $M_n = 6000$ ) and H2O using MDI or TDI, respectively. Both MDI and TDI are aromatic diisocyanates, their structure is typical.<sup>4</sup> The difference between MDI and TDI is that MDI has a more symmetrical structure and stronger rigidity but TDI has more side groups. Figure 6 is the DSC curves of HB-PU with various HSCs: (a) DSC pertaining MDI-HB-PU and (b) DSC pertaining TDI-HB-PU. The results are listed in Table II.

As shown in Table II, the crystallinity of pure PEG ( $M_n = 6000$ ) is 78.8%. The crystallinity of soft segment falls after putting in hard segment, because  $T_g$  and  $T_c$  of hard segment is higher than that of soft segment, the crystallization of soft segment is restrained by the hard segment. To this study, the critical  $M_n$  for the crystallization of soft segment may change with the types of hard segment; the critical  $M_n$  of soft segment with TDI hard segment is higher than with MDI hard segment.<sup>15–18</sup> This indicates that the crystallization of soft PEG segment has a bigger obstruction in TDI-HB-PU than in MDI-HB-PU. MDI-HB-PU have higher crystallinity and thermal storage property compared with TDI-HB-PU. This can be explained by the relative regular structure of MDI-H2O hard segment (Fig. 7). TDI has many side groups; its relative irregular structure decreases the two-phase-separation in TDI-HB-PU.

As seen in Figure 7 and Table II, the  $T_m$  and  $\Delta H_m$  of MDI-HB-PU and TDI-HB-PU decrease as HSC increases. This demonstrates that the size of micro-lite and the crystallinity of soft segment decrease when HSC increases. As the hard chain segment length becomes long, the degree of microphase-separation deepens. When the interaction between soft segment and hard segment is strengthened, more hard chain segments enter soft segment microdomains and the regularity of soft chain segments is

**TABLE II**  
Thermal Properties of PEG 6000 and HB-PU Measured by DSC Analysis

Samples		$\Delta H_m$ (J/g)	$T_m$ (°C)	$X_c$ (%)
PEG 6000	–	155.1	67.2	78.8
MDI-HB-PU	10% wt HSC	138.2	67.0	70.2
	20% wt HSC	118.1	64.4	60.0
	30% wt HSC	102.8	62.2	52.2
	40% wt HSC	91.2	57.5	46.3
TDI-HB-PU	10% wt HSC	126.7	66.9	64.4
	20% wt HSC	105.8	62.8	53.8
	30% wt HSC	82.7	60.9	42.2
	40% wt HSC	69.3	58.4	35.2

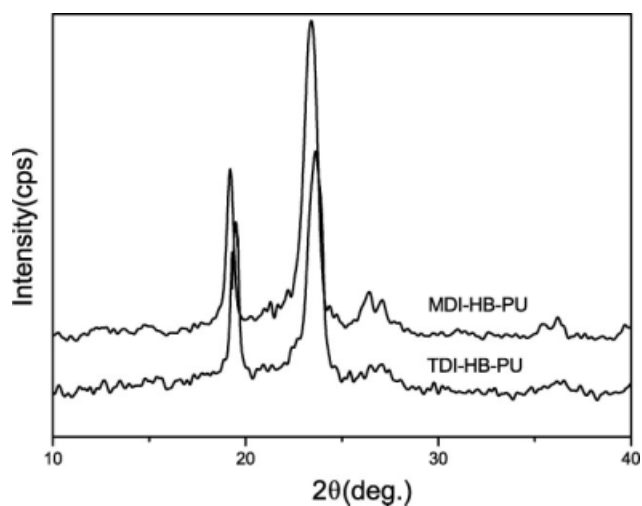


**Figure 7** Wide-angle X-ray diffraction patterns for the two HB-PU with 20 wt % hard segment content.

destroyed, which reduces the crystallinity of soft segment of HB-PU.

The influence of hyperbranched polyester polyalcohol with different functionalities

To discuss this influence, two families of HB-PU with various HSC using PEG ( $M_n = 6000$ ) as soft segment and TDI-H20 and TDI-H30 as hard segment were synthesized. Figures 8 and 9 display the relationship between the transition temperature (or enthalpy), and the SSC of the two families of HB-PU.

As shown in Figures 8 and 9, the transition temperature and enthalpy of the two families of HB-PU reduce with SSC decrease, but the H30-HB-PU decrease more quickly than the H20-HB-PU. The

DSC results show that the H20-HB-PU have higher crystallinity and phase separation than H30-HB-PU, which is attributed to the unique structure of the hyperbranched polyester polyalcohol. The length of branch, branch degree, and distribution can greatly affect the chemical, physical, mechanical, and rheological properties of hyperbranched polymers. At very high branching levels, the polymers prone to amorphous, the enthalpy associated with the melting transition decrease, and the  $T_m$  is lower due to the large number of short chain branches. Therefore, the percent crystallinity of polymers came down drastically with an increase in the branching content. These have been documented well in the literature elsewhere.<sup>19–21</sup> The effect of branching on rheological behavior has been investigated by other researchers.<sup>22</sup> For molecular weights higher than a critical value, the viscosity of the high branched molecule was higher than the low branched polymer, namely, the viscosity enhances as the degree of branching increases. Moreover, with the increase of the generation number of hyperbranched polyester polyalcohol, and the increase of the number of surface functional groups, the branch flexibility, especially chain end mobility increase and the inward folding of the molecules is more probable, the degree of chain entanglement decreases. This results in the assembly of hard segment domains and lower microarea separation. The crystallinity of PEG soft segments also decreases. Additionally, the extent of hydrogen-bonding between soft segment and hard segment in H30-HB-PU is widened, then the crosslinking density increases, this prevents the microarea separation of soft and hard segment too. Thus, the H20-HB-PU have higher crystallinity and better characteristic of heat storage than the H30-HB-PU.

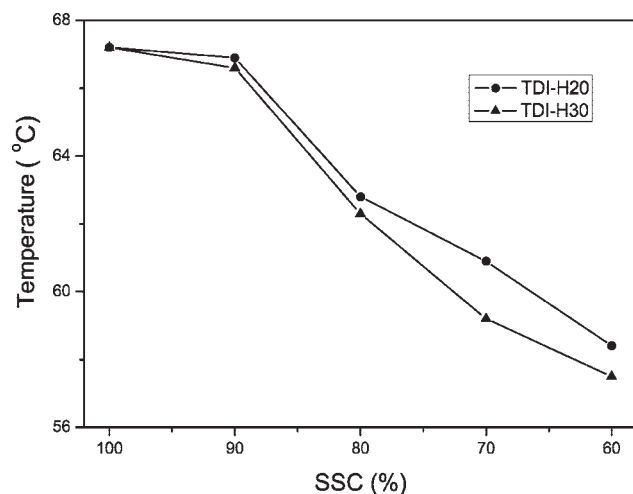


**Figure 8** Relationship curves between the transition temperature and the SSC of PEG for the two HB-PU.

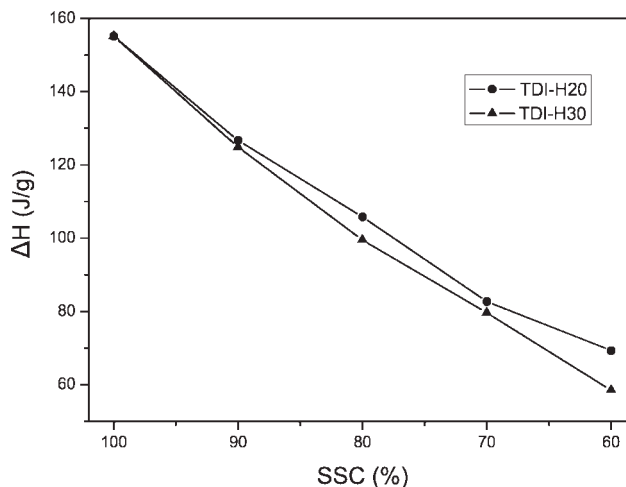


**Figure 9** Relationship curves between the enthalpy and the SSC of PEG for the two HB-PU.

### The influence of measure conditions on the crystallization of HB-PU

Two HB-PU, with 90 wt % and 70 wt % PEG 6000 soft segments, were prepared using MDI-H20 as hard segments. The crystallinity of the two HB-PU were measured by DSC using varying scanning rate. Results are shown in Figure 10 and Table III. The scanning rate shows great influence on the thermal properties of HB-PU. As the heating rate decreases, the  $T_m$  of the soft segment of HB-PU decreases but the  $\Delta H_m$  decreases only slightly. As the cooling rate decreases, the  $\Delta H_c$  decreases a little, whereas  $T_c$  increases significantly. Because of the strong temperature dependence of nucleation and crystal growth, a slow cooling rate provides better fluidity and diffusivity for molecules due to low viscosity and more time for crystallization, thus inducing higher crystallinity at higher temperature, than for a sample cooled with a fast cooling rate.

The results obtained from experimental data are treated with Avrami method reported in the litera-

**TABLE III**  
Thermal Properties of HB-PU Measured by DSC  
Analysis with Various Scanning Rates

Samples	Scanning rate (°C/min)	$T_m$ (°C)	$\Delta H_m$ (J/g)	$T_c$ (°C)	$\Delta H_c$ (J/g)
90 wt % SSC	5	63.1	137.1	40.6	127.7
	10	65.3	137.9	37.4	129.2
	15	66.1	138.0	34.2	130.3
	20	67.0	138.2	33.2	132.3
70 wt % SSC	5	57.3	100.5	31.7	98.2
	10	59.0	101.4	26.3	99.9
	15	60.9	102.0	22.4	100.6
	20	62.2	102.8	18.6	100.9

ture.<sup>23</sup> Classical Avrami equation can be used for nonisothermal crystallization analysis as follows:<sup>24</sup>

$$\log[-\ln(1 - X(t))] = \log K + n \log t$$

where  $X(t)$  is the relative crystallinity at time  $t$ ,  $K$  is a constant that is relevant to the nucleus formation, nucleation rate, and nucleus growth rate,  $n$  is Avrami exponent. The relation between the crystallization time  $t$  and the sample temperature  $T$  can be formulated as,

$$t = \frac{T_0 - T}{\Phi}$$

where  $\Phi$  is the cooling rate.

The plots of  $\log[-\ln(1 - X(t))]$  versus  $\log t$  for HB-PU with 90 wt % SSC and 70 wt % SSC are shown in Figure 11, respectively. Each curve shows the linear portion. Two adjustable parameters,  $K$  and  $n$ , can be obtained by linear regression are also listed in Table IV. It is clear that the faster the cooling rate, the larger the parameter  $K$  value is, implying there is more rapid crystallization rate. The  $n$  displays a range of values, HB-PU with 90 wt % SSC range from 2.63 to 3.16, and the 70 wt % SSC HB-PU varies from 2.08 to 2.94. As can be seen from the table, the simplified assumption that crystallization occurs under continuous temperatures is satisfied. The range of the  $n$  value is 2–3 suggests that the nonisothermal crystallization of HB-PU corresponds to three-dimensional growth with heterogeneous nucleation. As the SSC decrease, the  $n$  value decreases, which means that the crystallization process of HB-PU is affected by HSC.

### CONCLUSIONS

From the study it can be conclude that:

First, crystallization of soft segments and formation of microdomains and physical crosslinked point of hard segments are two necessary conditions for HB-PU having the characteristic of solid–solid phase

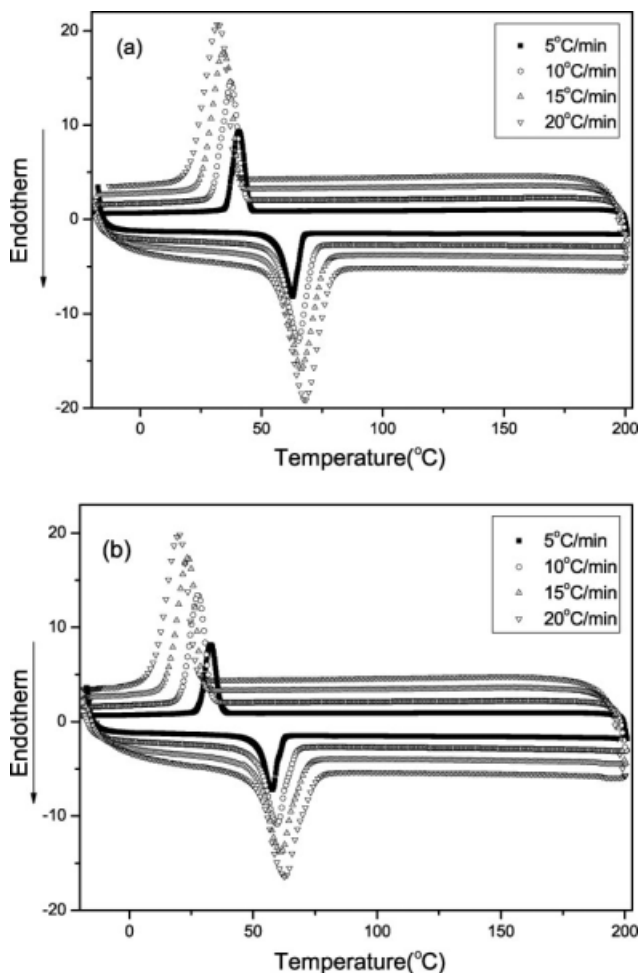


**Figure 10** Effect of scanning rate on DSC curves for HB-PU: (a) 90 wt % SSC and (b) 70 wt % SSC.

change for energy storage. Only when the  $M_n$  of PEG soft segment exceeds the critical value ( $M_n \geq 2000$ ), the soft segments can crystallize well and possess large phase change latent heat at room temperature.

Second, when the  $M_n$  of soft segment is above the critical  $M_n$  ( $M_n > 2000$ ), the increase of SSC and  $M_n$  of soft segment leads to the increase of phase transition enthalpy and phase transition temperature of HB-PU.

Third, hard segment has significant influence on the heat storage property of HB-PU. HB-PU with regular microstructure and lower generation of hyperbranched polyester polyalcohol have higher energy storage capability.

Fourth, the influence of measure conditions cannot be ignored.

All in all, via controlling soft segment molecule weight, SSC and hard segment structure, various

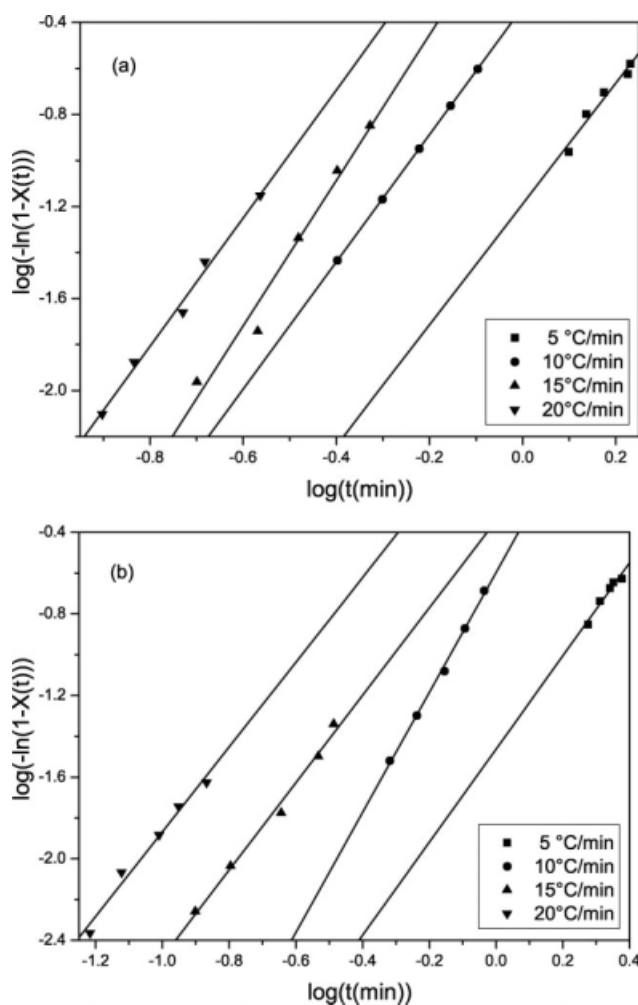


**Figure 11** Plots of  $\log[-\ln(1 - X(t))]$  versus  $\log t$  for HB-PU: (a) 90 wt % SSC and (b) 70 wt % SSC.

**TABLE IV**  
Parameters of Nonisothermal Crystallization Process of HB-PU with 90 wt % SSC and 70 wt % SSC

Samples	$\Phi$ ( $^{\circ}\text{C}/\text{min}$ )	$T_c$ ( $^{\circ}\text{C}$ )	$\log K$	$K$	$n$
90 wt % SSC	5	40.6	-1.19	0.06	2.63
	10	37.4	-0.33	0.47	2.77
	15	34.2	0.18	1.51	3.16
	20	33.2	0.42	2.63	2.79
70 wt % SSC	5	31.7	-1.46	0.03	2.28
	10	26.3	-0.60	0.25	2.94
	15	22.4	-0.34	0.46	2.14
	20	18.6	0.21	1.62	2.08

HB-PU solid–solid phase change materials suitable for heat storage can be obtained.

## References

- Shukla, A.; Buddhi, D.; Sawhney, R. L. *Renew Energy* 2008, 33, 2606.
- Hu, Y.; Rogunova, M.; Topolkaev, V.; Hiltner, A.; Baer, E. *Polymer* 2003, 44, 5701.
- Krzysztof, P.; Kinga, F. *Polym Adv Technol* 2005, 16, 127.
- Kang, W.; Stoffer, J. O. *Polym Prepr* 2000, 41, 1132.
- Li, Y.; Ren, Z.; Zhao, Z.; Zhao, M.; Yang, H.; Chu, B. *Macromolecules* 1993, 26, 612.
- Velankar, S.; Cooper, S. *Macromolecules* 1998, 31, 9181.
- Seefried, C. G.; Koleske, J. V.; Critchfield, F. E.; Dodd, J. L. *Polym Eng Sci* 1975, 15, 646.
- Bogart, J. W.; Gibson, P. E.; Cooper, S. L. *J Polym Sci Polym Phys Ed* 1983, 21, 65.
- Li, Y.; Kang, W.; Stoffer, J. O.; Chu, B. *Macromolecules* 1994, 27, 612.
- Martin, D. J.; Meijs, G. F.; Renwick, G.; Gunatillake, P. A.; Mccarthy, S.; Gunatillake, P. *J Appl Polym Sci* 1996, 62, 1377.
- Martin, D. J.; Meijs, G. F.; Renwick, G.; Gunatillake, P. A.; Mccarthy, S. *J Appl Polym Sci* 1996, 60, 557.
- Li, Y.; Gao, T.; Chu, B. *Macromolecules* 1992, 25, 1737.
- Chu, B.; Gao, T.; Li, Y.; Wang, J.; Desper, C. R.; Byrne, C. *Macromolecules* 1992, 25, 5724.
- Li, Y.; Gao, T.; Liu, J.; Lin, K.; Desper, R.; Chu, B. *Macromolecules* 1992, 25, 7365.
- Li, F.; Hou, J.; Zhu, W.; Zhang, X.; Xu, M.; Luo, X.; Ma, D.; Kim, B. K. *J Appl Polym Sci* 1996, 62, 631.
- Seefried, C. G. J.; Kolesk, J. V.; Critchfield, F. E. *J Appl Polym Sci* 1975, 19, 2493.
- Seefried, C. G. J.; Kolesk, J. V.; Critchfield, F. E. *J Appl Polym Sci* 1975, 19, 2503.
- Ping, P.; Wang, W.; Chen, X.; Jing, X. *Biomacromolecules* 2005, 6, 587.
- Jayakannan, M.; Ramakrishnan, S. *J Polym Sci Part A: Polym Chem* 2000, 38, 261.
- Fu, J. F.; Shi, L. Y.; Yuan, S.; Zhong, Q. D.; Zhang, D. S.; Chen, Y.; Wu, J. *Polym Adv Technol* 2008, 19, 1597.
- Ibnelwaleed, A.; Hussein, H. *J Appl Polym Sci* 2005, 97, 2488.
- Nakajima, N.; Yamaguchi, Y. *J Appl Polym Sci* 1996, 61, 1525.
- Xu, G.; Shi, W.; Hu, P.; Mo, S. *Eur Polym J* 2005, 41, 1828.
- Janimak, J. J.; Cheng, S. Z. D.; Zhang, A. Q.; Hsieh, E. T. *Polymer* 1992, 33, 728.